

AD 731 564

AFFDL-TR-70-146

PARAFOIL WIND TUNNEL TESTS

*JOHN D. NICOLAIDES
UNIVERSITY OF NOTRE DAME*

TECHNICAL REPORT AFFDL-TR-70-146

JUNE 1971

DDC
RECEIVED
OCT 28 1971
RESERVED
E

Approved for public release; distribution unlimited.

Reproduced by
NATIONAL TECHNICAL
INFORMATION SERVICE
Springfield, Va 22151

AIR FORCE FLIGHT DYNAMICS LABORATORY
AIR FORCE SYSTEMS COMMAND
WRIGHT-PATTERSON AIR FORCE BASE, OHIO

UNCLASSIFIED

Security Classification

DOCUMENT CONTROL DATA - R & D

(Security classification of title, body of abstract and indexing annotation must be entered when the overall report is classified)

1. ORIGINATING ACTIVITY (Corporate author) University of Notre Dame Notre Dame, Indiana		2a. REPORT SECURITY CLASSIFICATION UNCLASSIFIED	
		2b. GROUP N/A	
3. REPORT TITLE PARAFOIL WIND TUNNEL TESTS			
4. DESCRIPTIVE NOTES (Type of report and inclusive dates) Final Report			
5. AUTHOR(S) (First name, middle initial, last name) John D. Nicolaides			
6. REPORT DATE June 1971		7a. TOTAL NO. OF PAGES 201	7b. NO. OF REFS 18
8a. CONTRACT OR GRANT NO. AF33615-67-C-1670		9a. ORIGINATOR'S REPORT NUMBER(S) AFFDL-TR-70-146	
b. PROJECT NO. 6065		9b. OTHER REPORT NO(S) (Any other numbers that may be assigned this report)	
c. 606501			
d. 606501007			
10. DISTRIBUTION STATEMENT This document is subject to special export controls and each transmittal to foreign governments or foreign nations may be made only with prior approval of the Air Force Flight Dynamics Laboratory/AFR, Wright Patterson AFB, Ohio.			
11. SUPPLEMENTARY NOTES N/A		12. SPONSORING MILITARY ACTIVITY Air Force Flight Dynamics Laboratory Wright-Patterson AFB, Ohio 45433	
13. ABSTRACT Extensive Parafoil wind tunnel tests have been carried out by the University of Notre Dame in its 2 ft x 2 ft tunnel and in the NASA Langley 30 ft x 60 ft tunnel. Parafoil model sizes ranged from .09 ft ² to 147 ft ² and Parafoil aspect ratios ranged from .5 to 3.0. The wind tunnel test velocities ranged from approximately 20 ft per second to over 60 ft per second. The aerodynamic stability coefficients, C _L , C _D , C _M , C _{M₀} + C _{M₀} α, C _y , C _n , and C _l , were measured. The Parafoil remained self inflated and rigid over a range of angle of attack from -10° to 80° and revealed no stall characteristics. Maximum lift coefficients from 0.751 to 1.005 were measured for Parafoils of different aspect ratio. Maximum lift to drag ratios ranging from 1.83 to 6.40 were measured for the various Parafoil designs. The various wind tunnel tests confirm both the static and the dynamic stability of the Parafoil in pitch, yaw, and roll. The results of these investigations are consolidated in this report by summary plots and special presentations. Details of illustrations in this document may be better studied on microfiche			

DD FORM 1 NOV 65 1473

UNCLASSIFIED

Security Classification

NOTICES

When Government drawings, specifications, or other data are used for any purpose other than in connection with a definitely related Government procurement operation, the United States Government thereby incurs no responsibility nor any obligations whatsoever; and the fact that the Government may have formulated, furnished, or in any way supplied the said drawings, specifications, or other data, is not to be regarded by implication or otherwise as in any manner licensing the holder or any other person or corporation, or conveying any rights or permission to manufacture, use, or sell any patented invention that may in any way be related thereto.

FORM 28-100	
GROUP	NAME CODE
DOC	INT. SECTION
UNCLASSIFIED	CI
JUSTIFICATION	
BY	
DISTRIBUTION AVAILABLE BY CODE	
DIST.	AVAIL. AND SPECIAL
A	

Copies of this report should not be returned unless return is required by security considerations, contractual obligations, or notice on a specific document.

UNCLASSIFIED

Security Classification

14	KEY WORDS	LINK A		LINK B		LINK C	
		ROLE	WT	ROLE	WT	ROLE	WT
	Parafoil						
	Para-Foil						
	Steerable Parachute						
	Flexible Wing						
	Hi-Glide Canopy						
	Parachute						
	Gliding Parachute						
	Maneuverable Parachute						
	Parachute Wind Tunnel Tests						

UNCLASSIFIED

Security Classification

BLANK PAGE

PARAFOIL WIND TUNNEL TESTS

JOHN D. NICOLAIDES

Details of illustrations in
this document may be better
studied on microfiche

Approved for public release; distribution unlimited.

FOREWORD

This report was prepared by the University of Notre Dame, Notre Dame, Indiana, under U.S. Air Force Contract AF33615-67-C-1670. This contract was initiated under Project 6065, "Performance and Design of Deployable Aerodynamic Decelerators", Task 606501, "Terminal Descent Deceleration Concepts". The work was administered under the direction of the Recovery and Crew Station Branch of the Air Force Flight Dynamics Laboratory at Wright-Patterson Air Force Base, Ohio. Mr. R. Walker and Mr. R. Speelman served as successive project engineers during the duration of the effort.

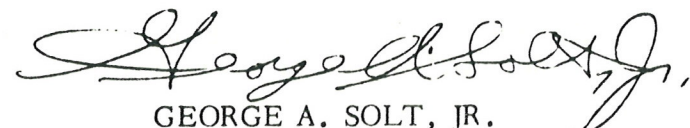
The author, of the University of Notre Dame Aerospace and Mechanical Engineering Department was J. D. Nicolaidis, Professor. Contributing students of the University of Notre Dame Aerospace and Mechanical Engineering Department were James Greco, Barney Goren, Charles Lorenzen, Steve Cuspard, Michael Tragarz, Michael Higgins and Patrick Sullivan.

The University of Notre Dame wishes to acknowledge the contributions of Mr. James Hassell, Jr. of NASA (Langley) in conducting the wind tunnel program, and in particular would like to acknowledge the extraordinary contributions of Mr. Ralph Speelman.

The contractor's number for this report is F33615-67-C-1670.

The manuscript for this report was released by the author in February 1971 for publication as an AFFDL technical report.

Publication of this report does not constitute Air Force approval of the report's findings or conclusions. It is published only for the exchange and stimulation of ideas



GEORGE A. SOLT, JR.
Chief, Recovery and Crew Station Branch
Vehicle Equipment Division
AF Flight Dynamics Laboratory

ABSTRACT

The first wind tunnel tests on the Parafoil were carried out at the University of Notre Dame beginning in 1964. Numerous designs were studied. Certain of these Parafoil configurations were of interest to the U. S. Air Force Flight Dynamics Laboratory, who sponsored the University in carrying out additional wind tunnel tests both at Notre Dame and at NASA Langley. The results obtained from these special wind tunnel tests, and from some of the original Parafoil tests are presented in this summary report. All of the Parafoil wind tunnel models tested in this program had a rectangular planform with aspect ratios ranging from .5 to 3.0 and with areas ranging from .09 ft² to 147 ft². The wind tunnel test velocities ranged from approximately 20 ft per second to over 60 ft per second. The wind tunnel tests also included studies of (1) numerous variations in the basic Parafoil configurations, (2) various flap deflections, (3) completely non-rigid models, (4) rigid models, (5) semi-rigid models, and (6) various rigging configurations. The lift and drag coefficients, C_L and C_D , were measured. The aerodynamic moment coefficient, C_m , was determined by both static and dynamic testing techniques. Also, the aerodynamic side force coefficient, C_y , the yaw moment, C_n , and the roll moment coefficient, C_l , were measured. The aerodynamic pitch damping moment coefficients, $C_{m\dot{\alpha}} + C_{m\dot{\alpha}}$, were measured by a unique dynamic testing technique. The wind tunnel tests results showed that the Parafoil is able to remain self inflated and rigid over a large range of angles of attack from -10° to 80° (maximum angle tested in the wind tunnel). The tests revealed that the lift curve slope was approximately linear over a large range of angles of attack, depending on the aspect ratio. None of the non-rigid Parafoil designs had the usual abrupt stall characteristics of the classical rigid airfoil. Also, the Parafoils retained a high lift coefficient over a very large range of angles of attack. Maximum lift coefficients from 0.751 to 1.005 are measured (no flap deflection). Maximum lift to drag ratios ranging from 1.83 to 6.40 were measured for various Parafoil designs. The various wind tunnel tests confirm both the static and the dynamic stability of the Parafoil in pitch, yaw, and roll.

The results of these investigations are consolidated in this report by summary plots and special presentations.

CONTENTS

	Page
INTRODUCTION	1
TESTING FACILITIES AND TECHNIQUES	3
Wind Tunnel Facilities	3
<u>Notre Dame Wind Tunnel</u>	3
<u>NASA (Langley) Full Scale Wind Tunnel</u>	3
Description of Models	3
<u>Notre Dame Models</u>	3
<u>NASA Langley Models</u>	6
Testing Techniques	7
<u>Notre Dame</u>	7
<u>NASA Langley (Series One)</u>	9
<u>NASA Langley (Series Two)</u>	9
<u>Tether Test Phase</u>	10
<u>Strut Testing Phase</u>	11
Data Reduction	12
<u>Notre Dame</u>	12
<u>Static Tests</u>	12
<u>Dynamic Tests</u>	12
<u>NASA Langley (Series One)</u>	14
<u>NASA Langley (Series Two)</u>	14

CONTENTS (continued)

	Page
ANALYSIS OF RESULTS	15
Early Notre Dame Tests	15
Early NASA Tests	17
Notre Dame Wind Tunnel Tests	17
<u>Notre Dame/Air Force Wind Tunnel Tests</u>	17
<u>Static</u>	17
<u>Dynamic</u>	17
NASA Langley Tests	18
<u>Qualitative</u>	19
<u>Comparison of Tether and Strut Data</u>	20
<u>Tether</u>	20
<u>Strut</u>	21
WIND TUNNEL TEST SUMMARY	22
Lift Summary	22
Lift to Drag Ratio Summary	22
Drag Summary	22
Moment Summary	22
PARAFOIL FLIGHT SYSTEMS	23
CONCLUDING REMARKS	23
APPENDIX	
I. Transformation of Moment Coefficients About	
Confluence Point	157

CONTENTS (continued)

Appendix	Page
<u>Longitudinal Stability</u>	158
<u>Directional Stability</u>	160
<u>Lateral Stability</u>	161
II Line Drag Analysis - Removal	166
<u>NASA-Langley (Series Two): Tether Phase</u> .	166
<u>NASA-Langley (Series Two): Strut Phase</u> .	168
<u>NASA-Langley (Series One)</u>	168
III Line Drag Analysis - Addition	172
<u>NASA-Langley (Series Two):Tether Phase</u> .	172
IV Notre Dame Model Drag Data Correction	173
V Parafoil Flight Performance	177
REFERENCES	183

ILLUSTRATIONS

Figure		<u>Page</u>
1	Para-Foil in Gliding Flight	24
2	Smoke Visualization in Notre Dame Wind Tunnel . . .	26
3	Schematic of Notre Dame Wind Tunnel	27
4	Notre Dame Wind Tunnel	28
5	Langley Full-Scale Tunnel	29
6	Para-Foil Model 1 Airfoil Section and Dimensions (in fraction of chord)	30
7	Para-Foil Model 2 Airfoil Section and Dimensions (in fraction of chord)	31
8	Para-Foil Model Assembly (Models 3 and 4)	32
9	Para-Foil Models 3 and 4 Airfoil Section and Dimensions (in fraction of chord)	33
10	Para-Foil Model 5 Airfoil Section and Dimensions (in fraction of chord)	34
11	Para-Foil Model 6 Airfoil Section and Dimensions (in fraction of chord)	35
12	Para-Foil Model 7 Airfoil Section and Dimensions (in fraction of chord)	36
13	Para-Foil Models 8-13 Airfoil Section and Dimensions (in fraction of chord)	37
14	Para-Foil Model 5 Dimensions in Inches	38
15	Para-Foil Model 6 Dimensions in Inches	39
16	Para-Foil Model 7 Dimensions in Inches	40

ILLUSTRATIONS (continued)

Figure		<u>Page</u>
17	Model 8: AR 1.0 (Dimensions in feet).	41
18	Model 9: AR 1.5 (Dimensions in feet).	43
19	Model 10: AR 2.0 (Dimensions in feet)	44
20	Model 11: AR 2.5 (Dimensions in feet)	45
21	Models 12 and 13: AR 3.0 (Dimensions in feet) . . .	46
22	Notre Dame Wind Tunnel with Static Test Mount Configuration	47
23	Para-Foil Model with Support Equipment as Mounted in Wind Tunnel Test Section.	48
24	Suspension System Components	49
25	Suspension System and Model Mounted on Wind Tunnel Door	50
26	Schematic of Polaroid Picture Showing α_T and γ . . .	51
27	Tether Testing Phase.	52
28	Strut Testing Phase	53
29 a	Tether Test Set-Up General Arrangement	54
29 b	Tether Test Set-Up - Mount Assembly	55
30	Strut Testing Phase	56
31 a	Strut AR 3.0 Model, $\alpha = -5^\circ$	57
31 b	Strut AR 3.0 Model, $\alpha = 7.5^\circ$	58
31 c	Strut AR 3.0 Model, $\alpha = 17.5^\circ$	59
32	Data Plot (Test No. 28).	60
33	Para-Foil Flow Visualization in Notre Dame Smoke Tunnel	61

ILLUSTRATIONS (continued)

Figure		<u>Page</u>
34	Early Notre Dame Tests: Summary Lift and Drag. . .	62
35	Early Notre Dame Tests: Summary Lift to Drag Ratio.	63
36	Rigid Airfoil with Model Variations	64
37	Rigid Para-Foil with Model Variations.	65
38	Early NASA Tests: Lift and Drag Summary	66
39	Early NASA Tests: Summary Lift to Drag Ratio	67
40	Early NASA Tests: Pitching Moment Summary	68
41	Early NASA Tests: Lateral-Directional Moment Summary.	69
42	Notre Dame 1967 Tests: Lift and Drag Summary Curves	70
43	Notre Dame 1967 Tests: Lift to Drag Ratio Summary Curves	72
44	Notre Dame 1968 Tests: Lift and Drag Summary	73
45	Notre Dame 1968 Tests: Summary Lift to Drag Ratio	74
46	Notre Dame 1968 Tests: Flap Deflection Summary Lift Curves	75
47	Variation of the Pitching Moment Stability Coefficient with Trim Angle.	76
48	Variation of Damping Moment Stability Coefficient with Trim Angle.	78
49	NASA Tether Tests: AR 1.0 Speed Summary	80
50	NASA Tether Tests: AR 1.5 Speed Summary	81
51	NASA Tether Tests: AR 2.0 Speed Summary	82

ILLUSTRATIONS (continued)

Figure		<u>Page</u>
52	NASA Tether Tests :AR 2.5 Speed Summary.	83
53	NASA Tether Tests: AR 3.0 Speed Summary.	84
54	NASA Tether Tests: AR Summary at 40 feet per second	85
55	C_L and C_D vs α . Tether Flap Deflection at 30 fps.	86
56	C_D & C_L vs α . Tether AR Model 1.0 with Leading Edge Opening Changed (without line drag)	88
57	L/D vs α . Tether AR 1.0 Model with Leading Edge Opening Changed (without line drag)	89
58	C_D & C_L vs α . Tether AR 3.0 Model w/Leading Edge Opening Changed (without line drag)	90
59	L/D vs α . Tether AR 3.0 Model with Leading Edge Opening Changed (without line drag)	91
60	C_L vs α . Strut AR Summary at 40 fps.	92
61	L/D vs α . Strut AR Summary without Line Drag at 40 fps.	93
62	C_m vs α . Strut AR Summary at 50 fps	94
63	AR Summary. Pitching Moment About the Confluence Point	95
64	$C_{L\alpha}$ per degree vs AR	96
65	$C_{n\beta}$ vs α . Strut Models at 40 fps	97
66	$C_{l\beta}$ vs α . Strut Models at 40 fps.	98
67	C_L vs α_s, α_v , Strut AR 2.0 Model.	99
68	L/D vs α_s, α_v , Strut AR 2.0 Model	100
69	Lift Coefficient: AR Summary	102

ILLUSTRATIONS (continued)

Figure		<u>Page</u>
70	Lift Curve Slope Summary. Lift Curve Slopes Brought Through Common Intercept at $\alpha = -5.0^\circ$	103
71	Aspect Ratio 0.5 Lift Coefficient Summary	104
72	AR 0.64 Lift Coefficient Summary	105
73	AR 0.78 Lift Coefficient Summary	106
74	AR 0.83 Lift Coefficient Summary	107
75	AR 0.94 Lift Coefficient Summary (Early NASA Tests)	108
76	AR 1.77 Lift Coefficient Summary	109
77	AR 1.0 Lift Coefficient Summary	110
78	AR 1.5 Lift Coefficient Summary	111
79	AR 2.0 Lift Coefficient Summary	112
80	AR 2.5 Lift Coefficient Summary	113
81	AR 3.0 Lift Coefficient Summary	114
82	Lift to Drag Ratio: AR Summary	115
83	AR 0.5 Lift to Drag Ratio Summary	116
84	AR 0.64 Lift to Drag Ratio Summary	117
85	AR 0.78 Lift to Drag Ratio Summary	118
86	AR 0.83 Lift to Drag Ratio Summary	119
87	AR 0.94 Lift to Drag Ratio Summary	120
88	AR 1.77 Lift to Drag Ratio Summary	121
89	AR 1.0 Lift to Drag Ratio Summary	122

ILLUSTRATIONS (continued)

Figure		<u>Page</u>
90	AR 1.5 Lift to Drag Ratio Summary	123
91	AR 2.0 Lift to Drag Ratio Summary	124
92	AR 2.5 Lift to Drag Ratio Summary	125
93	AR 3.0 Lift to Drag Ratio Summary	126
94	Drag Coefficient: AR Summary	127
95	AR 0.5 Drag Coefficient Summary	130
96	AR 0.64 Drag Coefficient Summary	131
97	AR 0.78 Drag Coefficient Summary	132
98	AR 0.83 Drag Coefficient Summary	133
99	AR 0.94 Drag Coefficient Summary	134
100	AR 1.77 Drag Coefficient Summary	135
101	AR 1.0 Drag Coefficient Summary	136
102	AR 1.5 Drag Coefficient Summary	137
103	AR 2.0 Drag Coefficient Summary	138
104	AR 2.5 Drag Coefficient Summary	139
105	AR 3.0 Drag Coefficient Summary	140
106	Drag Coefficient with Line Drag AR Summary	141
107	Lift to Drag Ratio with Line Drag: AR Summary	142
108	Lift to Drag Ratio with Line Drag: AR Summary	143
109	C _m vs α AR Summary Curves at 40 FPS	144
110	AR 1.0 C _m vs α	145

ILLUSTRATIONS (continued)

Figure		Page
111	AR 1.5 C_m vs α	146
112	AR 2.0 C_m vs α	147
113	AR 2.5 C_m vs α	148
114	AR 3.0 C_m vs α	149
115	AR 1.0 C_{mCPT} vs α	150
116	AR 1.5 C_{mCPT} vs α	151
117	AR 2.0 C_{mCPT} vs α	152
118	AR 2.5 C_{mCPT} vs α	153
119	AR 3.0 C_{mCPT} vs α	154
 Appendix		
I-1	Parafoil Axis System (Body Axes)	162
I-2	Axes Systems and Convention used to define positive sense of forces, moments, and angles. Longitudinal data are referred to wind axes and lateral data are referred to body axes	163
I-3	Longitudinal Stability Analysis Geometry	164
I-4	Directional and Lateral Stability Analyses Geometry Side Force Acting Downward at the Reference	165
II-1	Tether Testing Line Drag Determination	169
II-2	Sketch of Strut Test Configuration in Langley Full Scale Tunnel	170
IV-1	Protuberance Drag	174
IV-2	Summary of Coefficients of Drag (No Lines)	175
IV-3	L/D Summary No Lines	176
V-1	Line Drag Configuration AR 2.0	178

ILLUSTRATIONS (continued)

Figure		Page
V-2	C_L , C_D and L/D for AR 2.0 With Lines	179
V-3	C_L , C_D and L/D for AR 2.5 With Lines	180
V-4	C_L , C_D and L/D for AR 3.0 With Lines	181
V-5	C_L , C_D and L/D Summary - With Lines	182

NOMENCLATURE

a	Resultant force moment arm about quarter-chord reference
AR	Aspect ratio, ($=b/c$)
b	Parafoil span
c	Parafoil Chord: The distance along the bottom surface from the upper leading edge (projected down) to the trailing edge (Figure 6)
C_A	Axial force coefficient, $\frac{\text{Axial Force}}{qS}$
C_D	Drag coefficient of wing based on planform area, $\frac{\text{Drag}}{qS}$
$C_{D\pi}$	Drag coefficient of lines based on line area, $\frac{\text{Drag}}{qS_{\text{line}}}$
C_{DS}	Drag coefficient of lines based on wing planform area, $\frac{\text{Drag}}{qS}$
C_L	Lift coefficient, $\frac{\text{Lift}}{qS}$
$C_{L\alpha}$	Lift-curve slope, $\frac{\partial C_L}{\partial \alpha}$ per degree
C_l	Rolling-moment coefficient, $\frac{\text{Rolling Moment}}{q S_{\text{side}} b}$
$C_{l\beta}$	Lateral stability parameter, $\frac{\partial C_l}{\partial \beta}$ per degree
C_m	Pitching moment coefficient, $\frac{\text{Pitching Moment}}{qS c}$
$C_{m\alpha}$	Pitching stability parameter, $\frac{\partial C_m}{\partial \alpha}$ per degree
$C_{mq} + C_{m\dot{\alpha}}$	Aerodynamic pitch damping moment coefficients, $\frac{\text{Pitch Damping Moment} + \text{Lag Moment}}{qS c}$

NOMENCLATURE (continued)

C_N	Normal force coefficient, $\frac{\text{Normal Force}}{qS}$
C_n	Yawing-moment coefficient, $\frac{\text{Yawing Moment}}{qS_{\text{side}} b}$
$C_{n\beta}$	Directional stability parameter, $\frac{\partial C_n}{\partial \beta}$ per degree
C_R	Resultant force coefficient, $\frac{\text{Resultant Force}}{qS}$
C_y	Side force coefficient, $\frac{\text{Side Force}}{qS_{\text{side}}}$
D	Drag force
d	Distance parallel to Parafoil chord from lower leading edge to CPT
dia	Line diameter
FPS	Feet per second (fps)
ft	Feet
h	Vertical distance from platform to A-flare tip
I	Moment of inertia about Y axis (Pitch moment of inertia)
in	Inches
L	Lift force
\underline{L}	Length of A-suspension line from A-flare tip to attachment riser
l	Length from A-flare tip to extended platform line
L/D	Lift to drag ratio
M	Moment about pitch axis

NOMENCLATURE (continued)

mph	Miles per hour
n	Integer (number of ...)
q	Free-stream dynamic pressure
RN	Reynolds number
S, S _{wing}	Parafoil planform area, bc
S _{line}	Total line frontal area
t	Time (seconds)
V	Free-stream velocity
XYZ	Body axes (Figure I-1)
x	In longitudinal stability analysis: normal force moment arm about CPT
x	In tether line drag analysis: projected length along platform from CPT to A-suspension line
\bar{x}	Distance parallel to Parafoil chord from CPT to reference
x _{CP}	Distance parallel to Parafoil chord from reference to center of pressure
\bar{z}	Distance perpendicular to Parafoil chord, from CPT to Parafoil chord
α	Angle of attack of Parafoil chord line, lower surface of Parafoil, in degrees
α_s	Angle of attack determined by strut position
α_T	Trim angle of attack (Mean of the two extreme points of minimum amplitude)

NOMENCLATURE (continued)

α_v	Angle of attack determined by visual means
β	Angle of sideslip, in degrees
δ_f	Flap deflection parameter, positive when trailing edge is down
γ_l	Glide angle, $\arctan(C_D/C_L)$
γ	Angle between Parafoil chord line and suspension bars
θ_R	Angle of rigging, $\arctan(d/z)$
ξ	Length from Parafoil trailing edge to ring
\mathcal{Y}	Vertical distance from floor to strain gauge mount

SUBSCRIPTS

CPT	Confluence point
max	Maximum
NT	Nose taped
NNT	Nose not taped
REF	Reference point (also ref.)
sus	Suspension lines
cont	Control lines
guide	Guide lines
100	100 pound test line
375	375 pound test line
550	550 pound test line

MISCELLANEOUS

ND 1.67 (75) Notre Dame Parafoil of aspect ratio 1.67 and with an area of 75 ft²

INTRODUCTION

The Parafoil* is a true flying wing made entirely of nylon cloth and has absolutely no rigid members, Fig. 1. Like the aeroplane wing it has both an upper surface and a lower surface, and also an airfoil section. However the leading edge is open to permit self inflation due to ram air pressure. The Parafoil is composed of numerous airfoil shaped cells which give this cloth wing its unique rigid shape in flight. It is fabricated of a low porosity nylon cloth and can be packed and deployed in a manner similar to a conventional parachute. Flares or pennants are distributed along the bottom surface to which the various suspension lines are attached. These pennants serve three purposes: 1) they distribute the aerodynamic forces to the suspension lines, 2) they partially channel the flow into a two dimensional flow pattern which reduces tip losses and improves the aerodynamic efficiency and, 3) they provide side area which aids in obtaining directional flight stability.

The first wind tunnel tests on the Parafoil were carried out by Nicolaides^{1,2} in the unique flow visualization wind tunnels at the University of Notre Dame beginning in December of 1964, Fig. 2-4. Numerous Parafoil designs were studied which had variations in aspect ratio, airfoil section, planform, leading edge opening, trailing edge opening, pennant size-form-location, rigging, dihedral, wash-in, wash-out, et al. The data from these various wind tunnel tests revealed that the Parafoil had the same excellent aerodynamic characteristics as the classical rigid wing of aviation. This important finding was documented.¹⁶

Wind tunnel tests on the Parafoil carried out under the direction or cognizance of the University of Notre Dame include**:

- 1) Wind Tunnel tests at Notre Dame***
- 2) Wind Tunnel tests at NASA (Langley) Series 1. ****
- 3) Wind Tunnel tests at NASA (Langley) Series 2. ***

The results of all of these wind tunnel tests will be presented in this report together with some of the results from the original wind tunnel program.

*The Parafoil is a design and development of Dr. John D. Nicolaides (patent pending), and is based on the multi-cell ram airfoil Patent No. 3285546 held by SRRC, Inc., Florida.

**Professor J. D. Nicolaides, Principal Investigator.

***Supported by the Flight Dynamics Laboratory, U.S. Air Force, Wright Field.

****Supported by NASA (Langley). Two Parafoils furnished by Notre Dame.

Primary emphasis was placed on determining the static aerodynamic force coefficients, C_L and C_D , for various Parafoil configurations. The static aerodynamic moment coefficients, C_m , C_n , and C_l were also measured. The static side force coefficient, C_y , was measured. Of particular importance was the measurement of the damping and lag moment coefficients, $C_{m\dot{\alpha}} + C_{m\ddot{\alpha}}$, and the measurement of the static moment coefficient, $C_{m\alpha}$, from unique dynamic wind tunnel tests on a Parafoil model oscillating and damping in free pitching motion.

Numerous Parafoil configurations were tested which included variations in aspect ratio, airfoil thickness, airfoil shape, pennant design, leading edge opening, control surface deflections et al. Also, the tests were carried out for a wide range in Parafoil size, wind tunnel velocity, and rigging. The various data from these wind tunnel test programs will be presented. In order to assist the reader, special summary curves are presented which allow a definitization of Parafoil aerodynamics.

In the sections which follow the wind tunnel facilities and testing techniques will be reviewed, the various wind tunnel test results will be presented, and the general findings will be summarized.

TESTING FACILITIES AND TECHNIQUES

Wind Tunnel Facilities

Notre Dame Wind Tunnel

The University of Notre Dame wind tunnel is a low speed, indraft, and open circuit tunnel which has the characteristics summarized in Table I. Also see Figures 3 and 4. A series of anti-turbulence screens reduces the turbulence level of the air. A smoke generator provides white smoke when flow visualization is desired. Wind tunnel models 1-4 (Table II) were tested in the Notre Dame tunnel.

NASA (Langley) Full Scale Wind Tunnel

All NASA tests (series one and two) were carried out in the Langley Full-Scale Wind Tunnel, Langley, Virginia. The Langley Full-Scale Wind Tunnel is a low speed, double return and open test section wind tunnel with the characteristics given in the Table I. The tunnel and test section is illustrated in Figure 5. Models 5-13 were tested in the Langley tunnel (Table II).

Description of Models

Notre Dame Models

Model 1 (Table II) is one of the numerous original nylon fabric Parafoil scale models tested in the Notre Dame wind tunnels in the spring of 1965. The airfoil shape and dimensions are given in Figure 6.^{1,2}

Model 2, which was tested in the spring of 1966, is a rigid Parafoil model that was a replica of Parafoil number 125.* The dimensions of this model which was constructed in the Aero-Space Engineering Department of Notre Dame is given in Table II. Figure 7 gives the airfoil coordinates. The skin or covering of the model was 24 gauge aluminum sheet metal fastened to plexiglass ribs with an epoxy glue. The pennants were also made from 24 gauge aluminum sheet metal. In order to simulate the full-scale Parafoil a nylon cloth was laid over the aluminum upper surface.⁶

*Parafoil number 125 denotes a particular Parafoil known as "Notre Dame 2", which has an aspect ratio ($AR = \frac{b}{c}$) of 1.77 and a chord of 6 ft. 10 inches.

Table I
WIND TUNNELS

	Notre Dame	NASA (Langley)
V_{\max} :	90 fps	120 mph
Turbulence Level :	0.01%	1.1%
Test Section Shape :	2x2 ft (sq.)	30x60 ft (elliptic)
Test Section Length :	6 ft.	55.8 ft.
Contraction Ratio :	25:1	4.93:1
Horsepower :	15	8000

TABLE II
MODEL DESCRIPTION AND DIMENSIONS

<u>Model Number</u>	<u>Description</u>	<u>AR</u>	<u>Area</u>	<u>Chord</u>	<u>Maximum Thickness</u>
1	ND fabric scale model (Nicolaides-Knapp)	0.83	93.6 in ²	10.4 in.	.127C
2	ND rigid scale model (Nathe)	1.77	63.6 in ²	6 in.	0.19C @ 0.25C
3	ND semi-rigid model (Kang 1967)	3.0 2.5 2.0 1.5 1.0 0.5	75 in ² 62.5 50 37.5 25 12.5	5 in.	0.179C @ 0.21C " " " "
4	ND semi-rigid model (Kang 1968) (Walker)	3.0 2.5 2.0	75 62.5 50	5 in.	" " "
5	Fabric model (Langley Series One)	0.64	31.7 ft ²	7.04 ft	0.201C @ 0.25C
6		0.78	26.1	5.79	0.126C @ 0.25C
7		0.94	40.2	6.56	0.184C @ 0.25C
8	Fabric model (Langley Series Two)	1.0	147 ft ²	12.12 ft	0.179C @ 0.20C
9		1.5	"	9.00	"
10		2.0	"	8.57	"
11	"	2.5	"	7.67	"
12	"	3.0	"	7.00	"
13	Fabric model (Langley Series Two variable AR)	3.0 2.5 2.0 1.5 1.0	" 123 98 73.5 49	7.0 7.0 7.0 7.0 7.0	" " " " "

Models 3-4 are semi-rigid scale models constructed at the University of Notre Dame. The pennants and rib sections were made of galvanized iron (0.19 inches thick). The rib-only sections were made of aluminum shim stock of 0.01 inch thickness. The upper and lower surfaces were made of non-porous nylon cloth which was attached to the ribs with glue. Different aspect ratio models were formed by cutting off the end of the model at the rib-flare locations. Hence, these models can be referred to as the Notre Dame variable aspect ratio models. Model 3 yielded aspect ratios of 3.0, 2.5, 2.0, 1.5, 1.0, and 0.5 while model 4 resulted in aspect ratios 3.0, 2.5, and 2.0*. This latter aspect ratio of model 4 served as the test model for the dynamic test program.⁸ A schematic assembly of models 3 and 4 is given in Figure 8, while Figure 9 contains the airfoil coordinates.^{7,8}

NASA Langley Models**

Nine Parafoil models were tested, all employing a rectangular planform and a truncated airfoil shape with flat undersurface***. The airfoil section and dimensions of models 5-7 (series one) are given in Figures 10-12. The configuration and dimensions of models 8-13 (series two) are given in Figure 13. Model dimensions are given in Figures 14 - 16 for models 5-7; Figures 17-21 for models 8-13.

Structurally each model is composed of individual "air" cells sewn together. Each cell consists of a top cambered surface, a flat bottom surface, and airfoil section sides. Attached to the bottom surface are triangular shaped pennants to which the suspension lines are attached. The suspension lines are joined together at a confluence point located beneath the Parafoil. The position of the confluence point is determined from the desired trim angle and stability requirements for the Parafoil.

The confluence points of models 8-13 were determined to be 1.5 spans below the bottom surface and a distance forward determined by the testing mount arrangement.

Models 5-7 were made of approximately 2.0 oz. per square yard low porosity acrylic-coated, rip stop nylon. The suspension lines employed were of 375 pound test and 550 pound test braided nylon cord. The diameters of the lines were determined under tension to average approximately 0.125 inches (550 line) and 0.050 inches (375 line).

*Model 3 was tested in 1967; model 4 in 1968 under AFFDL contract.

**The NASA (Langley) Parafoil models were designed by Nicolaides and were constructed under the direction of the University of Notre Dame

***Models 5-7 were tested in the Spring of 1966. Models 8-13 were tested in March of 1968.

Model 13 was initially an aspect ratio three design with the same dimensions as model 12, however, in the test program side panels were subsequently cut off from each end reducing the aspect ratio in increments of 0.5, also affecting a reduction in planform area. Hence in the remainder of this analysis this model will be referred to as the Langley variable aspect ratio model.

Model 5 was procured from the Space Recovery and Research Center, Incorporated and models 6-7 were supplied by Nicolaides.³ Models 8-13 were supplied by the University of Notre Dame under contract to the Air Force.* The Dutron Corporation of South Bend fabricated the models.

Testing Techniques

Notre Dame

The Notre Dame static test models were supported vertically on a force balance system, located atop the test section as shown in Figure 22. This system uses a strain gauge balance to measure the lift and drag forces. The determination of the force coefficients from the strain gauge system will be treated in the section on data reduction. The angle of attack was recorded from a calibrated degree dial attached to the support sting atop the test section.^{1,6,7} In the early Notre Dame tests, a conventional rigid wing was tested, affecting a comparison between the Parafoil and the rigid airfoil. Since a Parafoil is made from nylon cloth and has pennants attached to its bottom surface, it was desired to establish the effects of these factors on aerodynamic performance. The conventional wing model (rigid airfoil) and the rigid Parafoil model were therefore each tested in the following manner:⁶

- (1) rigid model
- (2) rigid model plus pennants (flares)
- (3) rigid model plus nylon cloth
- (4) rigid model plus pennants plus nylon cloth

The pitching moment stability coefficient, $C_{m\alpha}$, and the pitch damping moment stability coefficient, $C_{m\dot{\alpha}} + C_{m\ddot{\alpha}}$, were measured by dynamic testing techniques in the Notre Dame⁹ tunnel.⁸ The techniques used consisted of photographing a pointer which was mounted to the supporting strut outside the top of the wind tunnel section as shown in Figure 23. The pointer oscillated with the same angular motion experienced by the Parafoil. The data points were read directly in degrees from the calibrated disk (referred to hereafter as the angle indicator) mounted under the pointer.

*Air Force Flight Dynamics Laboratory, Wright-Patterson Air Force Base, Contract No. F33615-67-C-1670, P002-P003.

The Parafoil was suspended from the axis of rotation by two steel bars as shown in Figure 24. These bars serve to simulate, in a completely rigid manner, the suspension lines of a Parafoil system in free flight. The suspension bars also allow for selecting various trim angles as well as various positions of the model above the axis of rotation.

The supporting strut was a 3/8 inch diameter steel rod, twenty-seven inches long with a needle point (7/16 inches) mounted on one end and separable into two sections to allow ease of installation and model position changes. A pointer was attached to that portion of the supporting strut which protruded outside and above the wind tunnel section. Figure 23 shows the pointer and angle indicator, which when photographed as it oscillates, provides support strut rotation in degrees.

The mounting arrangement for the support strut consisted of a low friction jewel bearing* in which the needle point rotated and two roller bearings prevented translation of the strut. The mounting system which contained these bearings was permanently attached to the door section of the wind tunnel as shown in Figure 25. This allowed ease of assembly and disassembly prior to and following each test sequence.

The Parafoil model was mounted in a four square foot working section (Sec. #8) as shown in Figure 23. Notice that the model is mounted in what is commonly referred to as the yaw plane.** Because the Parafoil was mounted in this fashion a glass bottom working section was used and each trim position as well as the angle between the suspension bars and the Parafoil chordline were obtained from a photograph taken through the bottom of the section as shown in Figure 26. A graphflex, still picture camera with polaroid attachment was used to take pictures of the Parafoil trim positions. From each picture the trim angle, α_T , and suspension bar chordline angle, γ , were obtained as also shown in Figure 26.

A 16mm high speed motion picture camera was mounted as shown in Figure 23. This camera ran at a film speed of 128 frames per second and photographed the pointer and angle indicator. The angular motions of the Parafoil were then read directly from the developed 16mm high-speed film.

The procedure used in acquiring the desired data after the test apparatus was assembled consisted of arbitrarily selecting a Parafoil trim position.

*The use of jewel bearings in this investigation reduces the friction to a negligible quantity. Any bearing friction in the support equipment would effect the damping moment coefficients, $C_{m\dot{\alpha}} + C_{m\ddot{\alpha}}$, but does not normally affect the frequency of oscillation and therefore does not affect the pitching moment coefficient, $C_{m\alpha}$.

**By mounting the model in this manner a gravity moment is not introduced when the trim angle of the model is changed.

This was achieved by fixing the angle between the suspension bars and the chordline after which the Parafoil assumed a trimmed condition (i.e. there were no moments about the pivot point). At this point a polaroid picture of the Parafoil was taken through the glass bottom of the test section. The Parafoil was then disturbed from its trim position by manually rotating the support strut (i.e. twisting by hand that portion of the strut which protruded through the top of the working section). Normally the Parafoil was displaced from its trim position approximately 8-10 degrees.

The support strut was then released at which time the high speed camera began photographing the pointer oscillations until they appeared to be completely damped. The time for the oscillations to damp varied from 8 to 15 seconds. Having completed these data acquisition requirements the entire procedure was repeated after selecting another trim angle which in effect simulated a different rigging of the Parafoil. Once a series of tests were completed for various trim angles, the Parafoil suspension system was disassembled and a change was made in the suspension bar length. This was accomplished by cutting the bars to a shorter length; thereby, simulating "different rigging" of the Parafoil by a method other than changing trim angle. With the shorter suspension bar the same procedure was used in obtaining the dynamics of the Parafoil at various trim positions. The Parafoil dynamics at three different suspension bar lengths were analyzed.

Following each test series and prior to shortening the suspension bars, the Moment of Inertia for that particular configuration was obtained.⁸

NASA Langley (Series One)

Four test set-ups³ were used in this technique in obtaining the aerodynamic data of models 5-7. The forces and moments acting on the Parafoils were measured by an externally mounted six-component strain gauge balance system. Reference 3 gives a detailed description of each technique incorporated.

Force tests were made over an angle of attack^{*} range from as low as 0° to as high as 70° to determine the static longitudinal stability characteristics of the models. The static lateral stability characteristics were measured over an angle of sideslip range from -10° to $+10^{\circ}$ and for angles of attack between 0° and 70° . Test wind tunnel velocities measured 20 to 40 feet per second.³

NASA Langley (Series Two)

The models were tested with two different mounting systems hereby referred to as (1) the Tether Testing Phase, and (2) the Strut Testing Phase. Figures 27 and 28 show photographs of the models as they appeared in each testing arrangement. The Tether Testing Phase yielded only the lift and drag coefficients of models tested, whereas the Strut Testing Phase provided the

^{*}See Nomenclature.

primary means for data acquisition of all the force and moment coefficients ($C_L, C_D, C_m, C_y, C_n, C_l$).

Tether Test Phase. Figures 29a and 29b illustrate the test set-up. The models were tested with its effective confluence point constrained. Since all suspension lines did not join at one point, the confluence point was considered to be the point where all the "front" lines were joined (effective confluence point). A strain gauge balance was mounted at this constraint measuring the lift and drag forces. The strain gauge-constraint was attached to a vertical I-beam and varied according to the aspect ratio model tested. This enabled the Parafoil to fly at the centerline of the tunnel. Table II-1 in Appendix II depicts the mount position per aspect ratio.

All the A-flare* suspension lines were brought together to a connector link, as were B, C, and D-flare suspension lines each to a connector link (Figure 29b). The four connector lines were then attached to four adjustable (web) risers. The risers were attached to a metal bar with connector links, with the bar attached to the strain gauge balance system.

The Parafoil model to be tested was raised into position by pulling upward on two "guide" lines (375# cord) attached to the forward outboard flare on each side. Once the model was elevated, the tunnel was turned on and gradually brought to the desired test speed. The two "guide" lines remained attached to the Parafoil and secured above the tunnel exit, but allowed slack so as to affect no additional constraint on the model. Control was maintained by employing an individual to operate the two control lines near the strain gauge balance. When the model appeared to be steady, the controller relaxed the controls and a data point was recorded. Simultaneously the angle of attack was obtained from the side by two techniques: (1) photographing the near side chord line and (2) visual inspection of the near side chord line, incorporating a window-mounted protractor in a plane parallel to the Parafoil chord line.

The angle of attack was varied by adjusting the position of the bar relative to the strain gauge mount, and, when necessary, the Parafoil profile was maintained by adjusting the risers. Due to limitations in the mounting system and the available wind tunnel area, the angles of attack ranged from 0° to 20° .

Tests were performed at tunnel speeds of 30, 40, 50 and 60 feet per second for models 9-12; tunnel speeds of 30, 40 and 50 feet per second for model 8; and speeds of 30 and 40 feet per second for the variable aspect ratio (Model 13). Each variable aspect ratio model was tested with its open leading edge taped 33%** (Figure 17a) closed and with a lighter line (100# test) replacing 75% of the heavier suspension lines (Figures 17-21). The variable aspect ratio 1.0 model was also tested with its nose untaped (to afford a comparison to the taped condition) and with the standard distribution of heavier line (Figure 17).

*Flare A is the leading edge flare, successive letters indicate successive flares proceeding toward the trailing edge of the canopy.

** A 1" width tape was placed in the center of each cell running from the top surface to the lower surface. The normal cell opening height defined the 100% tape length. Therefore the 33% length represented a cell decreased by 1/3.